JOURNAL OF RESEARCH of the National Bureau of Standards
Vol. 86, No. 3, May-June 1981

Absolute Determination of the Thermal Conductivity of Argon at Room Temperature and Pressures Up to 68 MPa

C.A.N. deCastro* and H.M. Roder**

National Bureau of Standards, Boulder, CO 80303

January 5, 1981

The thermal conductivity of argon at room temperature and for pressures up to 68 MPa has been measured with a transient hot-wire technique in order to assess the accuracy of an instrument of this type. The data are presented for a nominal temperature of 300.65 K and comparison with other authors shows that our data is accurate to within ± 1 percent, and it is the most accurate set of data for pressures above 35 MPa. Experimental evidence of a thermal conductivity enhancement near the critical density for a temperature about twice the critical temperature is herein reported. The experimental data were compared with the values predicted by the hard sphere model and it has been found that the theory gives values that are about 4 percent lower than the experimental ones in the density range 0–400 kg/m³ and about 1 to 2 percent lower in the high density region 400–825 kg/m³.

Key words: Ambient temperature; argon; critical enhancement; hard sphere; hot wire; thermal conductivity; transient

1. Introduction

Thermal conductivity of fluids has proved to be one of the most difficult transport properties to measure with a high accuracy, and only during the last decade has the development of the transient hot wire technique both for the gaseous phase [1–3][1] and liquid phase [4–6] made possible an accuracy of ± 0.3 percent for gases and ± 0.6 percent for liquids.

A new apparatus of the transient hot wire technique has been developed [7] to measure the thermal conductivity of fluids in the temperature range 70–320 K with pressure to 70 MPa. We report here the measurements obtained for argon at 300.65 K.

The purpose of this work is twofold: to assess the accuracy of the present instrument and to extend the pressure range of the high accuracy data obtained by Kestin, et. al. [2] at the same temperature. The extrapolation of our data to zero density coupled with the zero density viscosity obtained from the work of Kestin, et. al. [8] yields a value of the Eucken factor.

$$Eu = \frac{4\lambda_o M}{15 R \eta_o} \frac{f_\eta}{f_\lambda} = 1.0029 \qquad (1)$$

This in principle could support an uncertainty of not more than 0.3 percent. However, the precision of the experimental points is ± 0.6 percent when averaged over all densities and that suggests an overall accuracy of the data no better than ± 1.0 percent.

When we attempted to correlate the data with a low order polynominal

$$\lambda = \lambda_o + a_1 \varrho + a_2 \varrho^2 \qquad (2)$$

we obtained an S-shaped deviation plot which was clearly non-random. A detailed examination of the experimental data in the density range 5 to 15 mol/L (200 kg/m³ to 700 kg/m³) shows an anomalous increase in the thermal conductivity of up to 0.6 mW/m•K, which we attribute to a critical point enhancement even though the temperature is about twice the critical temperature.

To explore this unexpected behavior further we have applied the hard sphere model to the interpretation of the thermal conductivity of argon [9–11]. The difference between the experimental values and the calculated ones supports the existence of a critical point enhancement, as the hard sphere model agrees with the experimental values to within 0.7 mW/m•K or about 3.5 percent at densities below 5 mol/L and about 1.5 percent at densities above 15 mol/L. However, for densities between 5 and 15 mol/L where we find a critical enhancement the deviations run up to 1.35 mW/m•K, or about 5 percent. However, the magnitude of

*Centro de Quimica Estrutural, Instituto Superior Technico, 1096 Lisboa Codex, PORTUGAL

**Center for Chemical Engineering, National Engineering Laboratory

[1]Figures in brackets indicate literature references at the end of this paper.

the enhancement when established from a curve fit to the data is about 2.5 percent. Dymond [10], in an extension of the hard sphere model to dilute gases, found that for temperatures up to 1.7 T_c the thermal conductivities of argon determined by Michels, et al. [12] and Le Neindre, et al. [13] showed a similar critical enhancement, larger than the one reported here because of the lower temperatures involved. Dymond concluded that the hard sphere model is unable to account for the anomalous behavior of the thermal conductivity data.

2. The Principle of Operation

A detailed description of the hot-wire instrument will be given in a separate paper [7]; however, some of the more important details are given here.

For the transient hot-wire technique, a thin platinum wire immersed in the fluid and initially in thermal equilibrium with it, is subjected at time $t = 0$ to a step voltage applied to it. The wire will behave as a line source of heat with constant magnitude q.

The physical arrangement closely models an ideal line source, and the transient heat conduction equation, the temperature increase in the wire, ΔT is given by

$$\Delta T = \frac{q}{4\pi\lambda(T_r, \varrho_r)} \ell n \left(\frac{4K_o}{a^2 C} t\right) \tag{3}$$

where

$$T_r = T_o + \tfrac{1}{2}[\Delta T(t_1) + \Delta T(t_2)] \tag{4}$$

and

$$\Delta T = \Delta T_w - \Sigma\, \delta T_i \tag{5}$$

$K_o = \lambda(T_o, \varrho_o)/\varrho_o\, Cp_o$ is the thermal diffusivity of the fluid at the bath temperature when $t = 0$; a is the radius of the wire; and $\ell n\, C = \gamma$, where γ is Euler's constant. The times t_1 and t_2 are the initial and final times of measurement, and ΔT_w is the experimentally determined temperature rise in the wire. The corrections δT_i have been fully described elsewhere [1] and they account for the departure of the real instrument from the ideal model. Of these corrections the most important at lower times is δT_1, the effect of the finite heat capacity of the wire.

3. Description of the Instrument

Figure 1 shows the circuitry employed. Use of a Wheatstone bridge provides end effect compensation and follows the general development of the hot wire instrument pioneered by Haarman [14], de Groot, et al. [15], and Castro, et al. [16]. However, instead of measuring values of time corresponding to a bridge null with a fixed set of predetermined resistors, in the present instrument the voltage developed across the bridge is measured directly as a function of time with a fast response digital voltmeter (DVM). The DVM is controlled by a minicomputer which also handles the switching of the power and the logging of the data. The automation of the voltage measurement follows the work of Mani [17] who used a similar arrangement with a transient hot wire cell to measure resistance by the four lead technique rather than using a bridge.

Each arm of the bridge is designed to be 100 Ω, two arms R_1 and R_2 are standard resistors. The resistance in each of the other arms is a composite of the hot wire, leads into the cryostat and a ballast resistor. The ballast resistors allow each working arm to be adjusted to a value of 100 Ω.

The measurement of thermal conductivity for a single point is accomplished in two phases. In the first phase the bridge is balanced as close to null as is practical. With a very small applied voltage, 0.1 v normally, i.e., essentially at bath or cell temperature, the lead resistances are read on channels 1 and 7, the hot wire resistances on channels 3 and 4, and the ballast resistors on channels 2 and 5. For these measurements switch 1 is turned from dummy to the bridge while switch 2 is open. The ballasts are adjusted until each leg is approximately 100 Ω. Finally, with switch 2 closed, the bridge balance is checked on channel 6. The second phase incorporates the actual thermal conductivity measurement. The power supply is set to the applied power desired, switch 2 is closed, and switch 1 switched from dummy to bridge. The voltage developed across the bridge as a function of time is read on channel 6 and stored. The basic data is a set of 250 readings taken at 3 ms interval. Finally the voltage on channel 0 is read to determine the exact applied power. The cell temperature is found using a standard [18] arrangement of platinum resistance thermometer and six dial microvolt potentiometer. The pressure in the cell is read from a calibrated spiral steel bourdon tube using an associated optical read out. All of the pertinent data is written by the minicomputer onto a magnetic tape for subsequent evaluation. The cryostat, filling system, temperature controllers are described elsewhere [7].

An experimental run is a collection of individual points, usually an isotherm. For each run the data on the magnetic tape is processed point by point on a large computer. In addition to the reduction of the raw data, i.e., the conversion of bridge offset voltages to resistance changes and then to temperature changes of the wire, the set of 250 temperature changes is plotted as ΔT vs. $\ell n(t)$ for every point. The computer also evaluates the best straight line for the ΔT-$\ell n(t)$ data and determines the thermal conductivity $\lambda(T_r, \varrho_r)$ from the slope of this straight line. A second plot for every thermal conductivity point shows the "scattering

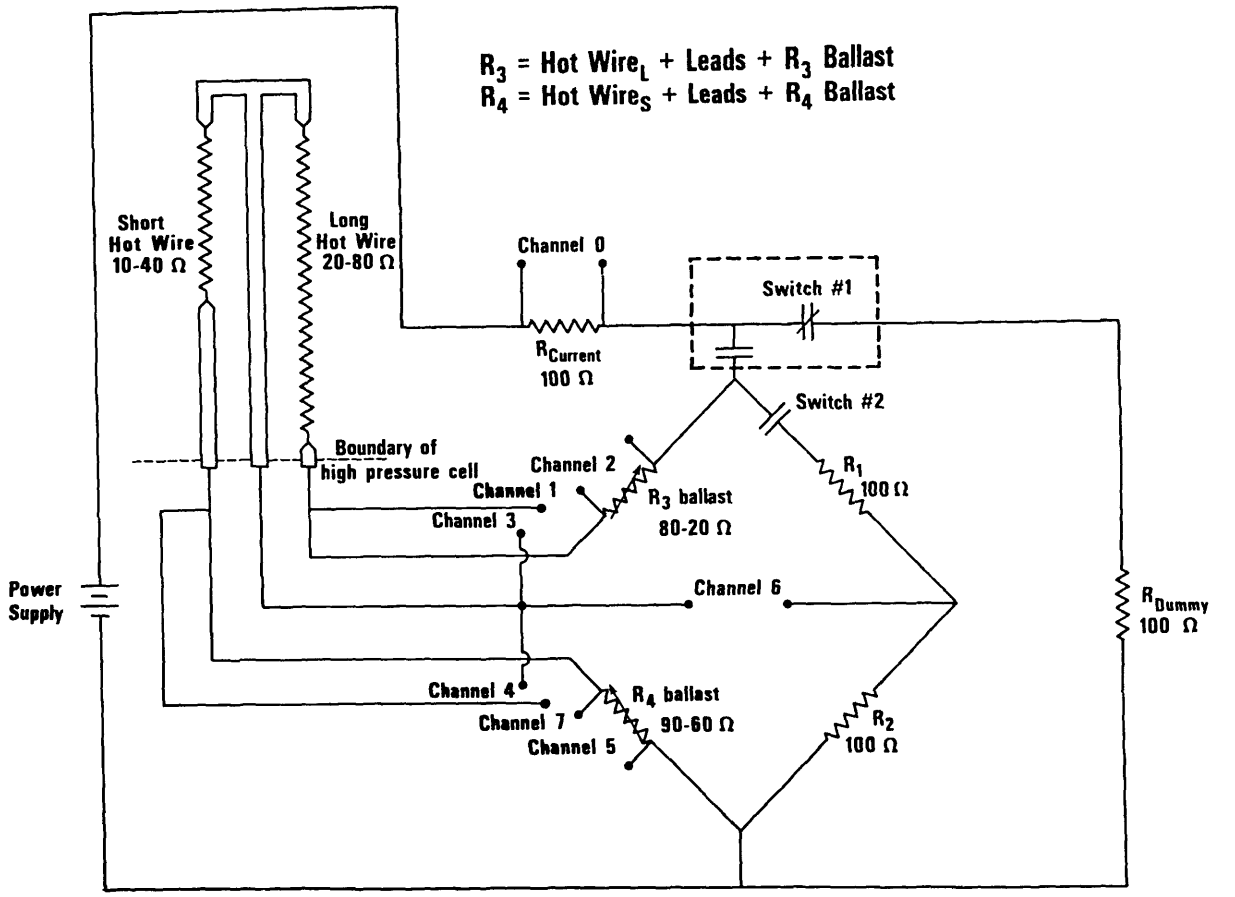

FIGURE 1. Circuit diagram of the hot wire apparatus.

diagram," i.e., the deviations of the set of 250 temperature changes from the calculated straight line.

4. Wire Calibration

In order to obtain the temperature increase of the platinum wires from the corresponding resistance increase, we need to know the variation of resistance with temperature for both wires. It has been shown in the past [4, 16, 19, 20] that an in situ calibration of the wires is desirable and also that the resistances per unit length of both wires must not differ by more than 2 percent. In addition, if they differ by more than 0.3 percent a correction to the temperature increase of the wire and to the heat generated in the long wire, functions of the resistances per unit length in both wires, must be applied [20].

The wire resistances measured at essentially zero applied power in the balancing of the bridge together with the cell temperatures as determined from the platinum resistance thermometer are taken as the in situ calibration of the wires. Some 1500 values were collected for each wire in the temperature range 150-320 K with pressures from atmospheric to about 70 MPa. The resistance relation for each wire is represented by an analytical function of the type

$$R(T) = A + B \cdot T + C \cdot T^2 + D \cdot P \qquad (6)$$

where T is the temperature in kelvin and P the gage reading. The pressure dependence is small but statistically significant and reflects the fact that the calibration measurements are made with a small applied power of 0.1 v. The constants obtained are presented in table 1. The long wire has a length of 10.453 cm at room temperature, the short wire one of 5.143 cm. Both wires have a nominal diameter of 0.00127 cm, thus the radius a in eq (3) is 0.000625 cm. Knowing that the length of both wires is a function of temperature, we can evaluate

$$\sigma_L = \frac{R_L(T)}{\ell_L(T)} \text{ and } \sigma_S = \frac{R_S(T)}{\ell_S(T)} \qquad (7)$$

and compare σ_L and σ_S in the experimental temperature range. Figure 2 shows the percent difference between σ_L and σ_S as a function of T and it can easily be seen that this

TABLE 1. *Calibration Constants of Wires*

	A/Ω	B/ΩK^{-1}	C/ΩK^{-2}	D/Ω (MPa)$^{-1}$	σ_0^*/Ωm^{-1}
Long wire	−9.065472	0.3534445	$-0.5923443 \times 10^{-4}$	-1.40146×10^{-3}	794.7
Short wire	−4.346459	0.1740251	$-0.2831553 \times 10^{-4}$	-6.56582×10^{-4}	798.8

σ_0^* is the resistance per unit length of each wire at 0.1 MPa and 273.15 K.

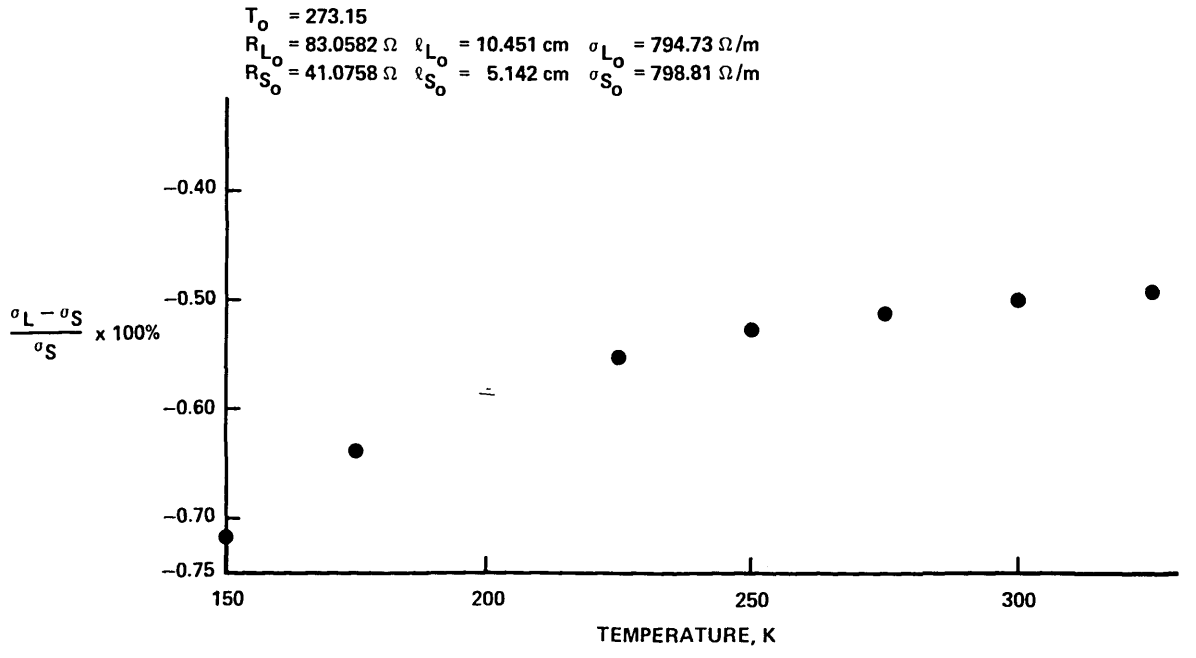

FIGURE 2. Wire calibration, resistance per unit length vs. temperature.

departure is no greater than 0.5 percent. The departure in figure 2 is as might be expected because the wires in the instrument were purposely left in the unannealed state. We are, therefore, justified in ignoring the correction proposed by Kestin and Wakeham [20].

5. Experimental Procedure

The wires and their supports are enclosed in a pressure vessel [7] which is operated at a nominal temperature of 296.1 K and controlled to within ± 0.002 K. The cell is filled with argon, maximum imprity 347 ppm, mostly oxygen. The gas was then compressed to about 70 MPa and allowed to cool to cell temperature before any measurements were taken. A series of measurements at different applied powers was made at a given level of pressure and then a small nearly isochoric expansion was made. The gas was allowed to warm up and reach equilibrium, then a new set of measurements at the new pressure level was taken. The applied power was varied in such a way that the total temperature increase in the wires ranged between 1 and 5 K. The time interval of measurement in the instrument can be varied, however we held the interval of measurement to 3 ms and the duration of the measurement to 0.75 s in order to avoid the onset of natural convection. The density of argon was taken from the equation of state developed at NBS [21, 22].

The total number of points taken was 112, with an average of four different power levels at each level of density or pressure. Overlap of density range in different working days was done to assess the longer term reproducibility of the instrument.

6. Performance of the Instrument

The analysis of the theory of the transient hot wire indicates that the corrected temperature rises of the wire ΔT must be a linear function of $\ell n(t)$ over the range of experimental measurements, provided that the instrument conforms to the ideal mathematical model.

Figure 3 shows the corrected temperature rises of the wires as a function of $\ell n(t)$, including the straight line fitted for a typical experimental point, 29062, in argon at the equilibrium temperature T_o = 300.168 K, and pressure, P = 18.879 MPa. Although the data set starts at 0.003 s, the plot begins at 0.033 s. In addition, it was found that the correction δT_1 was only of the order of 1 percent of ΔT for times around 0.15 s. At present no reliable correction δT_1 valid for $\delta T_1 > 1$ percent of ΔT is available. Therefore, the least squares straight line fitting considered only that part of the data set between times of 0.154 s and 0.755 s. Of the total of 250 individual measurements 200 are used in the fitting, the first 50 measurements are neglected. The onset of convection is determined as a deviation from the straight line at long times. Several trial runs established that for nearly all densities this process occurs around 1 s. However, at the very lowest densities measured the onset of convection occurs at experimental times less than 0.755 s, and for these points a second variable portion of the data set at long times had to be omitted from the least squares analysis.

Figure 4 shows the companion plot for point 29062, the deviations of the corrected temperature rises of the wires from the straight line fitting for that part of the data set between times of 0.033 s and 0.755 s. It is evident that for times valid in the least squares fitting, namely 0.154 s to 0.755 s, that data set departs by less than 0.8 percent from the regression line and that there is no evidence of a systematic curvature. A statistical evaluation of the error band for the slope of the least squares straight line is included in the output from the data reduction program.

To obtain the thermal conductivity from the slope we must use the value of q, the heat dissipation per unit length, which was found to be constant to within ± 0.1 percent during the measuring time.

The reproducibility of the instrument is obtained through an intercomparison of experimental points at the same nominal temperature and the same nominal density taken for different heat inputs. Table 2 shows one such set of experimental points obtained on two different days with different fillings at a density near 2.9 mol/L (116 kg/m³). The

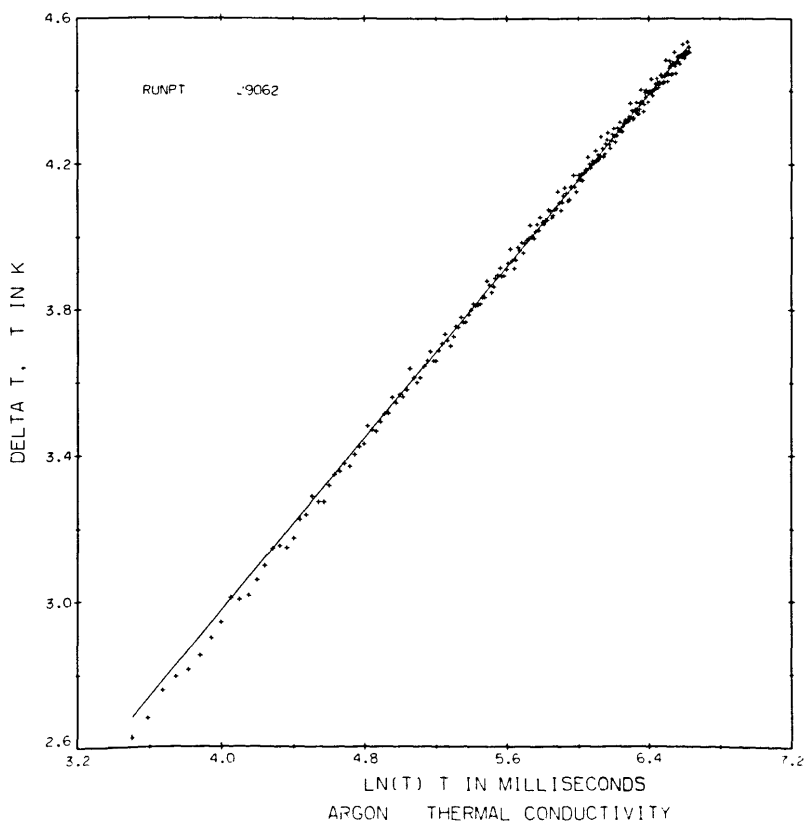

FIGURE 3. Typical rises in wire temperature vs. logarithm of time.

experimental thermal conductivities are adjusted a nominal temperature of $T_{nom} = 300.65$ K for the small temperature difference $T - T_{nom}$, following the argument that the excess thermal conductivity $\lambda(\varrho, T) - \lambda_0(0, T)$ is a function of density alone [2]. Hence

$$\lambda(T_{nom}, \varrho_r) = \lambda(T_r, \varrho_r) + \left(\frac{\partial \lambda}{\partial T}\right)_{\varrho, T_{nom}} (T_{nom} - T_r) \tag{8}$$

with

$$\left(\frac{\partial \lambda}{\partial T}\right)_{\varrho, T_{nom}} = \left(\frac{\partial \lambda_0}{\partial T}\right)_{T_{nom}} = 0.0501 \text{ mW/m•K}^2 \tag{9}$$

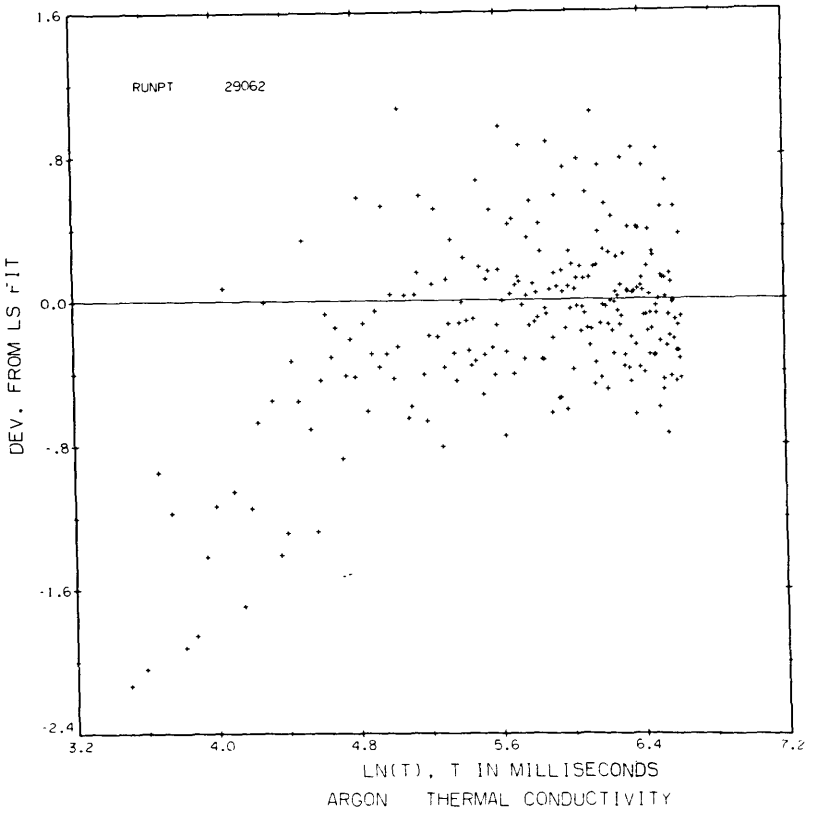

FIGURE 4. Typical deviations of the rise in wire temperature from the best straight line vs. logarithm of time.

TABLE 2. *Test of Reproducibility*

T_{nom} = 300.65 K ϱ_{nom} = 2.9 mol/L (116 kg/m³)

Run Pt	Pressure	T_r	Density	Thermal Conductivity W/m•K		
	MPa	K	mol/L	$\lambda(T_r, \varrho)$	$\lambda(T_{nom}, \varrho)$	$\lambda(T_{nom}, \varrho_{nom})$
29077	6.923	300.385	2.8572	.02044	.02045	.02049
29107	6.981	301.371	2.8706	.02054	.02050	.02052
29076	6.926	298.775	2.8772	.02034	.02043	.02045
29106	6.981	300.462	2.8812	.02041	.02042	.02043
29075	6.927	297.597	2.8914	.01997	.02012	.02013
29105	6.983	298.784	2.9015	.02024	.02033	.02033
29104	6.983	298.148	2.9090	.02024	.02037	.02036
29103	6.984	297.609	2.9161	.02026	.02041	.02040
						0.02039 ± 0.00012

The points are then further adjusted to an even density of 2.9 mol/L using a value of $(\frac{\partial\lambda}{\partial\varrho})T_{nom}$, ϱ_{nom} = 0.001 W•L/m•K•mol as shown in the last column of table 2. The average value for the eight points at T_{nom} = 300.65 K and ϱ_{nom} = 2.9 mol/L is 0.02039 ± 0.00012 W/m•K, the variance of this sample being ± 0.6 percent. The variance was found to be roughly the same for all densities, thus the precision of the instrument is on the order of ± 0.6 percent.

The accuracy of the instrument could be obtained from the value of the Eucken factor, equation (1), and the value obtained, 1.0029, through the extrapolated value of $\lambda(0, T_{nom})$ in a low density fitting of $\lambda(\varrho)$. However, considering the reproducibility to be ± 0.6 percent, and considering that the deviation of a set of ΔT data from its regression straight line is quite often closer to 0.8 percent, we shall regard the 0.3 percent obtained in the low density extrapolation as a fortunate coincidence, and claim an overall accuracy of ± 1 percent for the values of thermal conductivity.

7. Results and Analysis of the Data

Table 3 presents the 112 points obtained for argon in the density range 0.6 to 20 mol/L (24 to 820 kg/m³). The last column in table 3 shows the value of thermal conductivity adjusted to a nominal temperature of 300.65 K. Figure 5 shows the experimental values for the thermal conductivity of argon in the full density range and compares it with values by Kestin, et al. [2] (0-530 kg/m³), values by Michels, et al. [12] and values by Le Neindre, et al. [13]. The four sets of data agree within their mutual uncertainties of ± 1.0 percent, ± 0.3 percent, ± 2 percent and ± 3 percent respectively. Following the well known density dependence of thermal conductivity for moderately dense gases we tried to fit a curve of the type

$$\lambda = a_o + a_1\varrho + a_2\varrho^2 \qquad (10)$$

which is often used in place of the more rigorous expression, to our data. Initially we used the entire set of data, i.e., all densities up to 20 mol/L. Figure 6 shows the departure plot for this fit. Considering our precision to be ± 0.6 percent the S-shaped deviation shown in figure 6 is clearly nonrandom. This in turn implies that the functional form of the fitting function equation (10) is not appropriate. What is clear from this departure plot is that in order to get a valid extrapolation to zero density with a low order polynominal

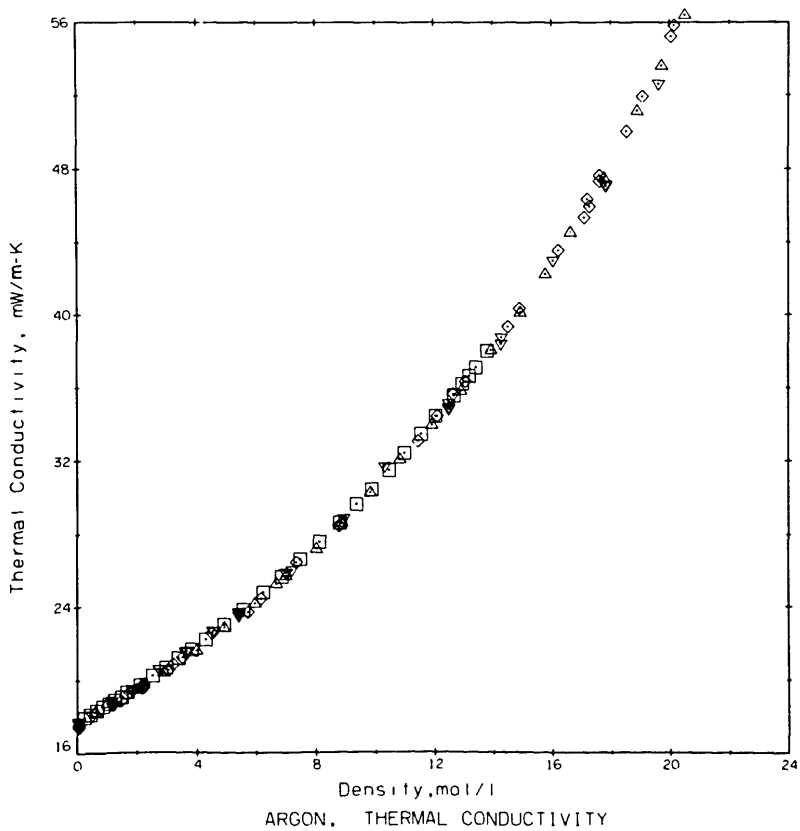

FIGURE 5. Thermal conductivity of argon at 300.65 K vs. density. △ this paper, ⊡ Kestin, et al. [2], ⊡ LeNeindre, et al. [13], ▽ Michels, et al. [12].

TABLE 3. *Experimental thermal conductivity values for argon.*

Run Pt	Press MPa	Temp K	Dens mol/L	Power W/m	ThermC W/m•K	Stat*	TC300.65 W/m•K
29123	1.461	304.195	.5811	.20246	.01835	.013	.01817
29122	1.462	301.738	.5863	.14149	.01830	.021	.01825
29121	1.462	299.669	.5905	.09143	.01804	.035	.01809
29120	1.462	298.025	.5939	.05225	.01832	.082	.01845
29084	2.412	300.384	.9759	.11518	.01869	.013	.01870
29083	2.413	299.468	.9794	.09146	.01868	.019	.01874
29082	2.413	298.709	.9824	.07048	.01874	.028	.01884
29081	2.414	297.883	.9856	.05227	.01839	.042	.01853
29119	2.996	309.226	1.1776	.35692	.01928	.004	.01885
29118	2.996	306.236	1.1904	.27420	.01906	.004	.01878
29117	2.996	303.507	1.2020	.20237	.01892	.007	.01878
29116	2.996	301.104	1.2125	.14150	.01879	.008	.01877
29115	2.996	299.370	1.2201	.09139	.01872	.027	.01878
29114	2.996	297.808	1.2271	.05224	.01841	.059	.01855
29080	4.758	299.859	1.9497	.11515	.01948	.014	.01952
29113	4.892	307.669	1.9476	.35706	.01964	.006	.01929
29079	4.759	299.059	1.9560	.09145	.01905	.019	.01913
29112	4.892	305.395	1.9642	.27417	.01989	.005	.01965
29078	4.760	297.714	1.9664	.05225	.01911	.043	.01926
29111	4.892	302.903	1.9827	.20239	.01968	.006	.01957
29110	4.892	300.779	1.9988	.14145	.01957	.010	.01956
29109	4.893	299.028	2.0126	.09141	.01936	.019	.01944
29108	4.893	297.710	2.0229	.05224	.01925	.043	.01940
29077	6.923	300.385	2.8572	.14146	.02044	.010	.02045
29107	6.981	301.371	2.8706	.17056	.02054	.008	.02050
29076	6.926	298.775	2.8772	.09145	.02034	.021	.02043
29106	6.981	300.462	2.8812	.14143	.02041	.009	.02042
29075	6.927	297.597	2.8914	.05225	.01997	.042	.02012
29105	6.983	298.784	2.9015	.09140	.02024	.020	.02033
29104	6.983	298.148	2.9090	.07040	.02024	.029	.02037
29103	6.984	297.609	2.9161	.05218	.02026	.045	.02041
29074	9.190	299.991	3.8313	.14153	.02137	.010	.02140
29073	9.194	298.556	3.8567	.09146	.02117	.021	.02127
29072	9.199	297.371	3.8787	.05223	.02114	.049	.02130
29102	9.686	300.836	4.0303	.17037	.02182	.008	.02181
29101	9.687	300.007	4.0450	.14130	.02177	.011	.02180
29100	9.688	298.560	4.0710	.09129	.02174	.022	.02184
29099	9.689	298.015	4.0810	.07035	.02155	.029	.02168
29071	11.609	301.155	4.8495	.20247	.02260	.009	.02257
29098	11.700	301.303	4.8851	.20215	.02298	.007	.02295
29070	11.612	299.541	4.8856	.14147	.02278	.014	.02284
29069	11.612	298.361	4.9116	.09132	.02276	.023	.02287
29097	11.701	299.745	4.9197	.14125	.02288	.012	.02293
29096	11.702	298.396	4.9499	.09129	.02270	.021	.02281
29095	13.812	301.069	5.7953	.20216	.02420	.011	.02418
29094	13.813	299.516	5.8370	.14128	.02381	.013	.02387
29068	14.183	300.847	5.9597	.20200	.02434	.008	.02433
29067	14.183	299.297	6.0025	.14120	.02418	.013	.02425
29066	14.184	298.105	6.0365	.09124	.02422	.024	.02435
29092	15.730	300.736	6.6210	.20216	.02525	.008	.02525
29089	15.732	299.969	6.6457	.17044	.02523	.009	.02526
29086	15.737	299.309	6.6687	.14132	.02531	.013	.02538
29085	15.772	299.555	6.6756	.14124	.02533	.013	.02538
29091	15.730	298.605	6.6875	.11497	.02512	.018	.02522
29087	15.734	298.011	6.7082	.09137	.02497	.025	.02510
29065	16.451	300.459	6.9344	.20198	.02572	.008	.02573
29064	16.454	299.103	6.9801	.14116	.02569	.013	.02577

TABLE 3. *Experimental thermal conductivity values for argon. (continued)*

Run Pt	Press MPa	Temp K	Dens mol/L	Power W/m	ThermC W/m·K	Stat*	TC300.65 W/m·K
29063	16.454	297.951	7.0184	.09124	.02544	.025	.02558
29062	18.879	300.168	7.9569	.20201	.02723	.008	.02725
29061	18.882	297.781	8.0498	.09124	.02694	.027	.02708
29060	21.041	301.382	8.7832	.27374	.02870	.006	.02866
29059	21.043	299.856	8.8475	.20206	.02851	.008	.02855
29058	21.044	298.723	8.8960	.14119	.02849	.015	.02859
29018	23.481	302.213	9.6941	.35561	.02983	.005	.02975
29057	23.679	300.997	9.8244	.27376	.03054	.006	.03052
29056	23.681	299.696	9.8854	.20201	.03018	.008	.03023
29055	23.682	298.414	9.9462	.14116	.03022	.016	.03033
22054	26.202	300.783	10.7689	.27371	.03205	.007	.03204
29053	26.205	299.445	10.8368	.20205	.03196	.010	.03202
29052	26.208	298.337	10.8942	.14121	.03155	.017	.03167
29014	26.498	300.188	10.9051	.27320	.03235	.006	.03237
29051	29.172	300.418	11.8240	.27533	.03427	.007	.03428
29050	29.174	299.255	11.8868	.20201	.03350	.011	.03357
29012	29.462	300.076	11.9397	.27324	.03409	.013	.03412
29049	29.177	298.195	11.9450	.14116	.03358	.018	.03370
29011	29.464	297.705	12.0688	.14100	.03390	.018	.03405
29048	32.339	300.161	12.8650	.27378	.03576	.006	.03578
29047	32.342	298.995	12.9312	.20207	.03562	.011	.03570
29046	32.342	298.097	12.9820	.14118	.03577	.018	.03590
29045	35.633	301.174	13.7911	.35636	.03803	.005	.03800
29044	35.634	299.942	13.8620	.27378	.03780	.007	.03784
29008	35.944	300.660	13.9090	.35592	.03844	.006	.03844
29004	35.943	300.636	13.9100	.35603	.03833	.005	.03833
29043	35.636	298.805	13.9281	.20213	.03780	.012	.03789
29007	35.944	299.506	13.9755	.27344	.03759	.009	.03765
29042	35.639	297.878	13.9832	.14124	.03764	.019	.03778
29003	36.014	299.434	13.9995	.27348	.03783	.008	.03789
29002	35.943	297.991	14.0633	.20171	.03830	.012	.03843
29001	35.941	297.734	14.0779	.14120	.03750	.019	.03765
29005	35.943	297.481	14.0932	.14107	.03832	.020	.03848
29041	39.399	300.710	14.8433	.35650	.04009	.006	.04009
29040	39.401	299.670	14.9047	.27378	.04012	.008	.04017
29039	39.401	298.695	14.9622	.20205	.04014	.012	.04024
29038	39.403	297.775	15.0174	.14124	.03978	.021	.03992
29036	42.981	300.625	15.7366	.35638	.04202	.006	.04202
29037	42.978	299.395	15.8087	.27389	.04225	.009	.04231
29035	42.983	298.473	15.8648	.20211	.04220	.013	.04231
29033	46.726	300.320	16.6035	.35637	.04445	.007	.04447
29034	46.723	299.253	16.6659	.27382	.04455	.009	.04462
29032	46.729	298.283	16.7252	.20204	.04430	.011	.04442
29031	52.190	300.095	17.7302	.35635	.04735	.006	.04738
29030	52.190	298.226	17.8407	.20206	.04748	.013	.04760
29029	58.578	300.830	18.8360	.44999	.05099	.004	.05098
29028	58.578	299.852	18.8926	.35636	.05117	.007	.05121
29027	58.580	298.024	19.0000	.20199	.05113	.016	.05126
29026	63.535	299.687	19.7015	.35602	.05357	.007	.05362
29025	63.538	298.024	19.7983	.20189	.05343	.016	.05356
29024	68.709	300.446	20.4228	.45004	.05638	.005	.05639
29023	68.710	299.553	20.4738	.35661	.05604	.008	.05609
29022	68.710	298.724	20.5213	.27399	.05621	.010	.05631
29021	68.709	298.014	20.5620	.20224	.05637	.017	.05650
29020	68.709	297.413	20.5966	.14140	.05642	.030	.05658

*The data reduction program determines both a value for the slope and its uncertainty, i.e., slope = S ± 2.1 σ. Printed here is STAT = 2.1 σ/S.

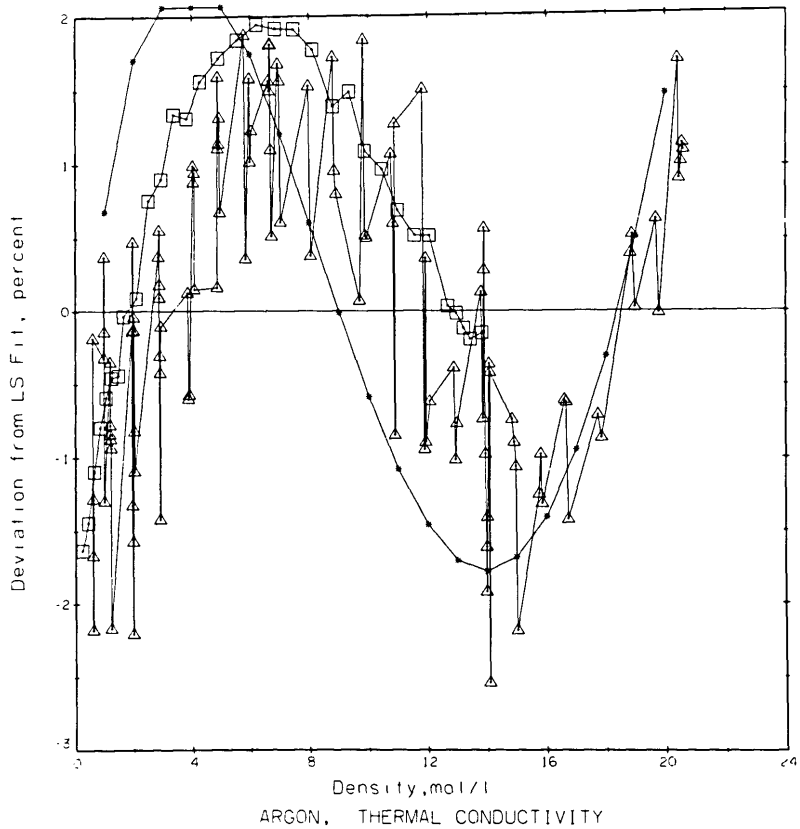

FIGURE 6. Deviations of the curve fit of equation 10 for the entire range of densities vs. density. △ this paper, ⊡ Kestin, et al. [2], * Hanley, et al. [22].

we should fit to densities no higher than about 7 mol/L, i.e., the first 56 points only of table 3. The departure plot for a fit over this reduced range in density is shown in figure 7. In this plot the departures are indeed random as the one sigma and two sigma error bands show. Table 4 shows the coefficients obtained for both density ranges including the statistical errors of the coefficients. Included for comparison in figures 6 and 7 are the experimental thermal conductivities of Kestin, et al. [2] and the values predicted by the correlation of Hanley, et al. [22]. The latter is based on the data reported by Michels, et al. [12] and Le Neindre, et al. [13].

We propose that there is an anomalous increase in the thermal conductivity which we attribute to a critical enhancement even though the temperature here T_{nom} = 300.65 K is about twice the critical temperature. To prove the existence of an enhancement we did a special curve fit to which the following considerations applied: (1) we will constrain the isotherm through the proper zero density value; (2) we will use a functional form that is appropriate, yet is also highly constrained; (3) looking at figure 6 we will fit only data between 0 and 7 mol/L as well as data above 14 mol/L in density and look at the deviation plot for densities between 7 and 14 mol/L. The equation selected has been used with some success to separate the background thermal conductivity from the critical component (see for example ref. 22).

$$\lambda = A + B\varrho + C\left\{e^{D\varrho} - 1.0\right\} \qquad (11)$$

In the fit to be described A is constrained to be 0.01783 W/m•K, D is a fixed value of 0.060 while B and C are treated as parameters to be determined. The cutoff points in density actually used are 5 and 15 mol/L and the deviation plot of this fit is shown in figure 8. The plot shows that the deviations for densities between 0 and 5 mol/L and between 15 to 20 mol/L are random, and it clearly illustrates the nature and size of the enhancement. In particular, figure 8 shows that the enhancement is several times larger, about 2.5 percent, than the precision inherent in our measurements, ± 0.6 percent.

8. The Rigid Hard Sphere Calculations

In order to look at the proposed enhancement from a different point of view we note that Dymond [9] in applying the

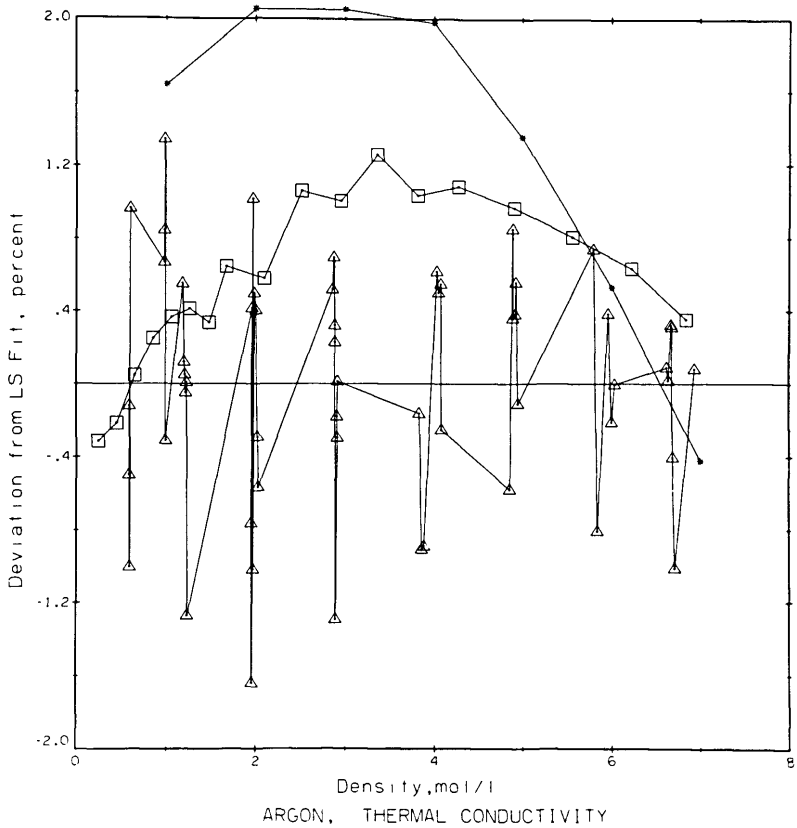

FIGURE 7. Deviations of the curve fit of equation 10 for the low density range only vs. density. △ this paper, ⊡ Kestin, et al. [2], * Hanley, et al. [22]. The error band of this fit is $\sigma = 0.51$ percent.

TABLE 4. *Coefficients of Least Squares Fittings*

Equation	Density Range of Fit mol/L	a_0 W/m•K	a_1 W•L/m•K•mol	a_2 W•L²/m•K•mol²	Average Deviation From Fit, Percent
10	0-20	$0.18089\times10^{-1}\pm0.16\times10^{-3}$	$0.63372\times10^{-3}\pm0.41\times10^{-4}$	$0.58497\times10^{-4}\pm0.20\times10^{-5}$	for 112 points 0.92
10	0-7	$0.17836\times10^{-1}\pm0.12\times10^{-3}$	$0.69942\times10^{-3}\pm0.82\times10^{-4}$	$0.62858\times10^{-4}\pm0.11\times10^{-4}$	for 56 points 0.51
		Fixed	Variable, B W•L/m•K•mol	Variable, C W/m•K	(Number of Points Fitted is 63)
11	0-5 and 15-20	A=0.01783 W/m•K D=0.060 L/mol	$-0.31015\times10^{-3}\pm0.38\times10^{-4}$	$0.18511\times10^{-1}\pm0.35\times10^{-3}$	for 63 points 0.54 for 112 points 0.88

hard sphere theory to dense and dilute gases, found evidence that the thermal conductivity data of argon and krypton shows an enhancement for temperatures up to 1.7 T_c which could not be represented by theory. We thus decided to apply the Van der Waals model to our data to see if a similar discrepancy could be noted at even higher temperatures. Use of the hard sphere model satisfies one of the considerations above, it supplies a functional form that is appropriate, yet highly constrained.

The Van der Waals model for transport properties of fluids is equivalent to a hard sphere model with a slightly temperature dependent hard core diameter, $\sigma_{HS}(T)$. It is a model that corrects Enskog's [23] expressions for the density dependence of the transport properties of a hard sphere fluid for both velocity correlations in the dense gas and for the attractive forces important in dilute gas collisions [9-11].

Enskog [23] based his equations on the assumption of molecular chaos and arrived at a value for the dense gas thermal conductivity given by:

$$\frac{\lambda_E}{\lambda_o} = \frac{1}{g(\sigma)} + 1.2\left(\frac{b}{V}\right) + 0.755\, g(r)\left(\frac{b}{V}\right)^2 \qquad (12)$$

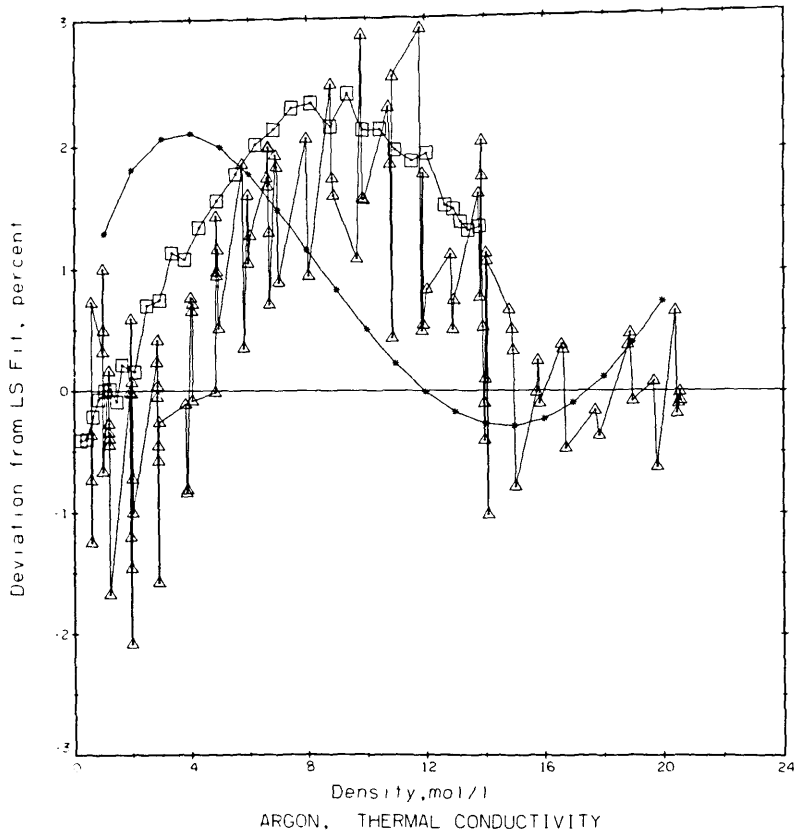

FIGURE 8. Deviations of the curve fit of equation 11 vs. density. The actual fit is limited to values between 0 and 5 mol/L as well as values between 15 and 20 mol/L. △ this paper, ⊡ Kestin. et al. [2], * Hanley, et al. [22].

where λ_o is the thermal conductivity of the low density gas of hard spheres, given by

$$\lambda_o = \frac{75}{64}\left(\frac{K^3 T}{\pi m}\right)^{1/2} \frac{1}{\sigma_{HS}^2} \tag{13}$$

$g(\sigma)$ is the radial distribution function at contact. For a system which can be approximated as given by Alder, et al. [11] the $g(\sigma)$ becomes

$$g(\sigma) = \frac{(1 - y/2)}{(1 - y)^3} \tag{14}$$

with

$$y = \frac{b}{4V} = \frac{1}{6}\pi \frac{N}{V}\sigma_{HS}^3 \tag{15}$$

the other symbols have the usual meaning.

Dymond [9] found that for high densities, where $\frac{V_o}{V} > 0.3$, V_o being the closed packed volume ($V_o = N\sigma_{HS}^3/2$), the Enskog values should be corrected for the molecular correlated motions and using molecular dynamics formulation he obtained

$$\left(\frac{\lambda}{\lambda_E}\right)_{MD} = 1.02 + 0.1\left[\frac{V_o}{V} - 0.3\right]; \frac{V_o}{V} > 0.3 \tag{16}$$

For the dilute and dense gas the expression has to be modified because the attractive forces do play an important role in heat conduction. Dymond [10] arrived at an expression, a function of the ratio T_c/T that it is supposed to account for the effect, the full expression being

$$\frac{\lambda_{HS}}{\lambda_E} = \left(\frac{\lambda}{\lambda_E}\right)_{MD} - \left[0.355 - 2.0\left(\frac{V_o}{V}\right) + 2.7\left(\frac{V_o}{V}\right)^2\right]\left(\frac{T_c}{T}\right)^{1/2}$$

$$\text{for } \frac{V_o}{V} < 0.3 \tag{17}$$

We have applied equations (12) to (17) to calculate the thermal conductivity of argon at $T = 300.65$ K as a function of

density, using a value of $V_o = 3.299 \times 10^{-4}$ m³/kg interpolated from Dymond's data of V_o as a function of temperature [10].

Figure 9 shows the comparison between our smoothed experimental thermal conductivity values and the values predicted by the hard sphere theory, λ_{HS} as a function of the ratio V_o/V. It can be seen that theory predicts the thermal conductivity of argon to within 0.7 mW/m•K (about 3.5 percent at low densities and 1.5 percent at high densities).

Figure 10 shows the difference between λ_{exp} and λ_{HS} as a function of density and it can be seen that the critical enhancement in the experimental data occurs near the critical density.

This comparison seems to support the existence of a critical enhancement in thermal conductivity even at temperatures around twice the critical temperature, a result that can only be detected if the accuracy of the thermal conductivity measuring method is sufficiently high.

9. Conclusions

This paper presents experimental data of the thermal conductivity of argon at 300.65 K from low density to 68 MPa obtained with a transient hot wire instrument.

The precision of the measurements is ± 0.6 percent while the accuracy of the data is estimated to be ± 1.0 percent. However, an Eucken factor of 1.0029 was obtained.

A small critical enhancement of about 2.5 percent was found in the experimental data between 0.34 ρ_c and 1.13 ρ_c, that has not been reported before. Comparison with values calculated from the hard sphere model shows that this model cannot predict the enhancement.

Our results agree with those of Kestin, et al. [2], Michels, et al. [12] and Le Neindre, et al. [13] within the mutual uncertainty.

The results confirm that the instrument is capable of measuring thermal conductivity of dense fluids with an accuracy of ± 1.0 percent. We expect to report results on helium, oxygen and propane in the near future.

One of us (CANC) is grateful for and wishes to acknowledge financial support from NATO Grant 1874 and would also like to thank the Luso-American Cultural Commission for a Fulbright-Hays travel grant. Our work was partially supported by NASA under Purchase Request C-32369-C.

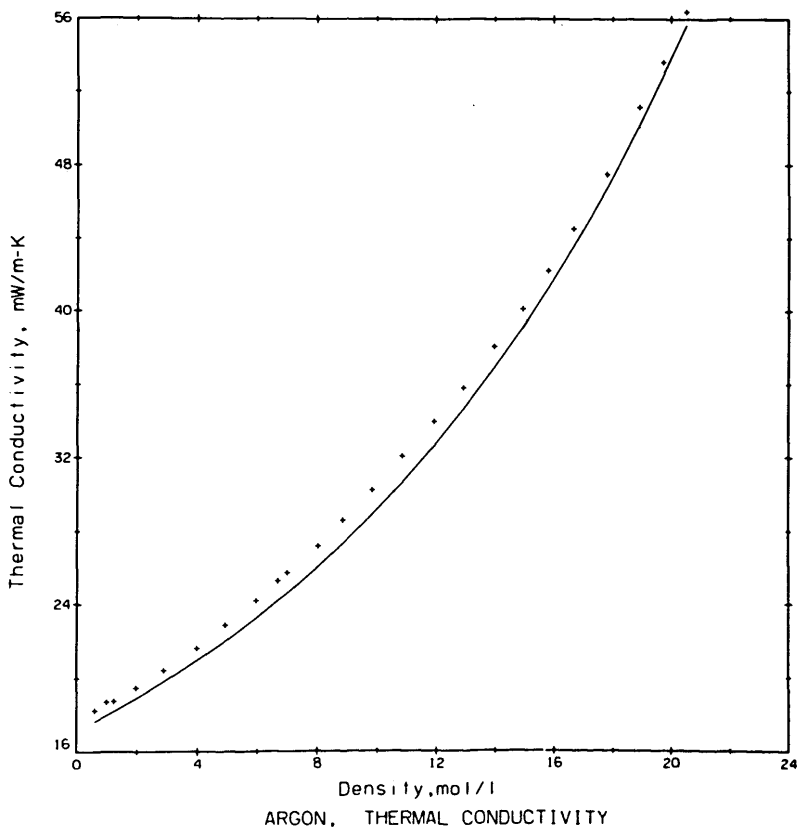

FIGURE 9. Calculated hard sphere and smoothed experimental thermal conductivities vs. density.

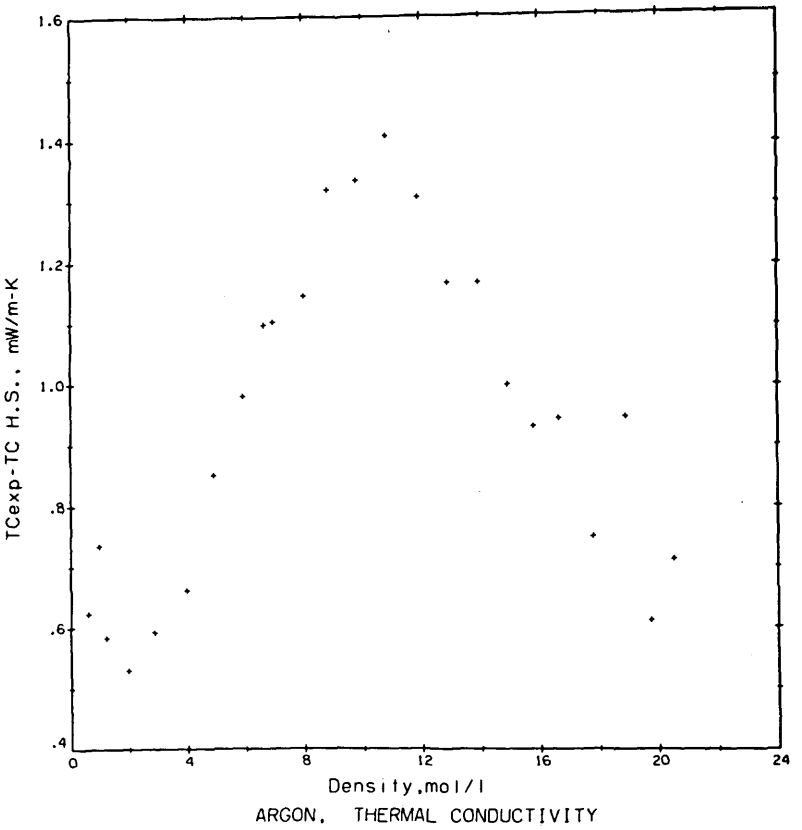

FIGURE 10. Differences between smoothed experimental and calculated hard sphere thermal conductivities vs. density.

10. References

[1] Healy, J. J.; de Groot, J. J.; Kestin, J. The theory of the transient hot-wire method for measuring thermal conductivity. Physica. **82C**(2): 392-408; 1976 April.

[2] Kestin, J.; Paul, R.; Clifford, A. A.; Wakeham, W. A. Absolute determination of the thermal conductivity of the noble gases at room temperature up to 35 MPa. Physica. **100A**(2): 349-369; 1980 February.

[3] Assael, M.J.; Dix, M.; Lucas, A.B.; Wakeham, W.A. Absolute determination of the thermal conductivity of the noble gases and two of their binary mixtures. J. Chem. Soc., Faraday Trans. **77**(1): 439-464; 1981.

[4] de Castro, C. A. Nieto; Calado, J. C. G.; Wakeham, W. A. Absolute measurements of the thermal conductivity of liquids using a transient hot-wire technique. Cezarilyan, A. ed. Proceedings of the seventh symposium on thermophysical properties; 1977 May 10-12; Gaithersburg, Maryland; New York; ASME; 1977; 730-738.

[5] de Castro, C. A. Nieto; Calado, J. C. G.; Wakeham, W. A. Thermal conductivity of organic liquids measured by a transient hot-wire technique. High Temperatures-High Pressures. **11**: 551-559; 1979.

[6] Menashe, J.; Wakeham, W. A. Absolute measurements of the thermal conductivity of liquids of pressures up to 500 MPa. to be published, Physica.

[7] Roder, H. M. A transient hot wire thermal conductivity apparatus. to be published, J. Res. Nat. Bur. Stand. (U.S.).

[8] Kestin, J.; Ro, S. T.; Wakeham, W. A. Viscosity of the noble gases in the temperature range 25-700 °C. J. Chem. Phys. **56**(8): 4119-4124; 1972 April 15.

[9] Dymond, J. H. The interpretation of transport coefficients on the basis of the van der Waals model. I. Dense fluids. Physica. **75**: 100-114; 1974.

[10] Dymond, J. H. The interpretation of transport coefficients on the basis of the van der Waals model. II. Extension to dilute gases. Physica. **79A**(1): 65-74; 1975 January-March.

[11] Alder, B. J.; Gass, D. M.; Wainwright, T. E. Studies in molecular dynamics. VIII. The transport coefficients for a hard sphere fluid. J. Chem. Phys. **53**(10): 3813-3826; 1970 November 15.

[12] Michels, A.; Sengers, J. V.; Van de Klundert, L. J. M. The thermal conductivity of argon at elevated densities. Physica. **29**: 149-160; 1963.

[13] Le Neindre, B.; Bury, P.; Tufeu, R.; Johannin, P.; Vodar, B. Recent developments at Bellevue on thermal conductivity measurements of compressed gases. Flynn, D. A.; Peavy, B. A., Jr. ed. Thermal conductivity; Proceedings of the seventh conference; 1967 November 13-16; Gaithersburg, Maryland. Nat. Bur. Stand. (U.S.) Spec. Publ. 302; 1968 September. 579-593.

[14] Haarman, J. W. Thesis. Technische Hogeschool; Delft; 1969.

[15] de Groot, J. J.; Kestin, J.; Sookiazian, H. Instrument to measure the thermal conductivity of gases. Physica. **75**: 454-482; 1974.

[16] de Castro, C. A. Nieto; Calado, J. C. G.; Wakeham, W. A.; Dix, M. An apparatus to measure the thermal conductivity of liquids. Journal of Physics E: Scient. Inst. **9**: 1073-1080; 1976.

[17] Mani, N. Precise determination of the thermal conductivity of fluids

using absolute transient hot-wire technique. Thesis. University of Calgary. Calgary, Alberta, Canada. 1971 August.

[18] Goodwin, R. D. Apparatus for determination of pressure-density-temperature relations and specific heats of hydrogen to 350 atmospheres at temperatures above 14°K. J. Res. Nat. Bur. Stand. (U.S.) **65C**(4); 231-243; 1961 October-December.

[19] de Castro, C. A. Nieto; Wakeham, W. A. Experimental aspects of the transient hot-wire technique for thermal conductivity measurements. Mirkovich, V. V. ed. Thermal conductivity 15. 1977 August 24-26; Ottawa, Ontario, Canada; New York; Plenum Publ. Corp.; 1978; 235-243.

[20] Kestin, J.; Wakeham, W.A. A contribution to the theory of the transient hot-wire technique for thermal conductivity measurements. Physica. **92A**(1 & 2): 102-116; 1978 June.

[21] An equation of state for argon, based on the work of Gosman, A. L.; McCarty, R. D.; Hust, J. G. Thermodynamic properties of argon from the triple point to 300 K at pressures to 1000 atmospheres. Nat. Bur. Stand. (U.S.) Nat. Stand. Ref. Data Ser. 27; 1969 March. 146 p. The functional form of the equation and the pertinent coefficients are given in reference 22.

[22] Hanley, H. J. M.; McCarty, R. D.; Haynes, W. M. The viscosity and thermal conductivity coefficients for dense gaseous and liquid argon, krypton, xenon, nitrogen and oxygen. J. Phys. Chem. Ref. Data. **3**(4): 979-1017; 1974.

[23] Enskog, D. Kinetische Theorie der Wärmeleitung, Reibung und Selbstdiffusion in gewissen verdichteten Gasen und Flüssigkeiten. Kungl. Svenska Vetenskapsakademiens Handlingar. **63**(4): 1-44; 1922.